Biochimica et Biophysica Acta, 376 (1975) 63–71

BBA 46860

THE IRON ELECTRON-NUCLEAR DOUBLE RESONANCE (ENDOR) OF 4-Fe CLUSTERS IN IRON–SULFUR PROTEINS FROM *CHROMATIUM* AND *CLOSTRIDIUM PASTEURIANUM*

R. E. ANDERSON[a], G. ANGER[a], L. PETERSSON[a], A. EHRENBERG[a,*] and R. CAMMACK[b], D. O. HALL[b], R. MULLINGER[b] and K. K. RAO[b]

[a]*Department of Biophysics, Stockholm University, Arrhenius Laboratory, S-104 05 Stockholm (Sweden) and* [b]*Department of Plant Sciences, King's College, 68 Half Moon Lane, London SE24 9JF (U.K.)*

(Received August 6th, 1974)

SUMMARY

Iron electron-nuclear double resonance (ENDOR) measurements were made of the 4-Fe clusters in oxidized *Chromatium* high-potential iron–sulfur protein, dithionite-reduced high-potential iron–sulfur protein in 80 % dimethylsulphoxide, fully reduced *Clostridium pasteurianum* ferredoxin in aqueous solution and in 80 % dimethylsulfoxide. The hyperfine couplings determined show that: i) the electron distribution in each case is nearly symmetric; ii) there are two types of iron in oxidized high potential iron–sulfur protein; iii) only one type of iron is observed in each fully reduced 4-Fe cluster; iv) the data also suggest a greater electron delocalization onto the ligands as compared to the 2-Fe ferredoxins.

INTRODUCTION

The class of iron–sulfur proteins containing 4-Fe clusters has been studied by EPR [1, 2], Mössbauer [2–4], NMR [5–7], and most importantly X-ray crystallography [8, 9]. The crystallographic data show that the cluster has an iron atom at each of the four alternate corners of a distorted cube, each iron being bound to a cysteine sulfur and the nearest three of the four inorganic sulfur atoms which occupy the remaining corners of the cube. This structure is present in the high-redox-potential iron–sulfur protein from *Chromatium* [8], which has a molecular weight of 10 000, with four iron and four labile sulfur atoms per molecule; and in the low-potential eight-iron ferredoxin from *Peptococcus aerogenes* [9], which has a molecular weight of 6 000, with eight iron and eight sulfur atoms arranged in two identical clusters, 12 Å apart. In each known case, the cluster dimensions are identical within the 2-Å measurement accuracy. The same structure is assumed valid for the 4-Fe ferredoxins

Abbreviation: Me_2SO, dimethylsulfoxide.

* To whom correspondence should be addressed.

(e.g. those from *Bacillus polymyxa* and *Bacillus stearothermophilus*) and the 8-Fe ferredoxin from *Clostridium pasteurianum*.

The magnetic properties of the cluster are summarized at a yet primitive level by a three-oxidation-state hypothesis of Carter et al. [10] in which each state differs by one electron per cluster. Thus, oxidized high-potential iron–sulfur protein is in State C^+ and is paramagnetic with $S_{eff} = \frac{1}{2}$, resulting in an apparently axial EPR spectrum with $g_{\parallel} = 2.12$ and $g_{\perp} = 2.04$, although additional spectral structure suggests a second EPR component. Mössbauer spectroscopy does not display more than one valence state but there is evidence for two hyperfine fields of opposite sign, indicating antiferromagnetic exchange coupling [3, 11]. The single electron reduction of high-potential iron–sulfur protein results in a diamagnetic state designated C, which according to the theory is equivalent to the oxidized ferredoxin state. Reduction of this state by a single electron for each 4-Fe cluster results in a State C^- for both the normal 4- and 8-Fe ferredoxins and the low-potential (so-called "super reduced") [12] state of high-potential iron–sulfur protein.

The EPR spectra of separate 4-Fe clusters in the reduced state, C^-, such as super-reduced high-potential iron–sulfur protein, the 4-Fe ferredoxins, and partially reduced 8-Fe ferredoxins (in which only one centre is paramagnetic) are all similar and nearly axial. The EPR spectra of fully reduced 8-Fe ferredoxins, such as that from *C. pasteurianum* are more complex, apparently due to inter-cluster spin–spin couplings [2], (see also ref. 1, p. 238). If the reduced ferredoxin molecule is unfolded by treatment with dimethylsulphoxide (Me_2SO) the EPR spectrum reverts to the simpler type, with axial symmetry, implying that interactions between the two clusters are prevented (R. Cammack, unpublished observations).

The Mössbauer spectra of *C. pasteurianum* ferredoxin display a single average valence state in both oxidation states.

MATERIALS AND METHODS

Instrumentation

The normal Varian E9 ENDOR–EPR spectrometer was used throughout except that the radio frequency oscillator and amplifier were replaced by a Telonic Model 2003, and ENI Model 3102, respectively. In place of a normal sine-wave field modulation, large amplitude (100–200 G p.p. 35 Hz) square-wave modulation was provide by switching a d.c. power supply (Oltronix B60-15R) which drove two external modulation coils (200 turns of 0.7-mm wire) mounted on the pole caps. The rise time is approx. 1 ms and an effective inhomogeneity of about 3 G.

The normal Varian wide-access cavity was used together with a Scanco (James F. Scanlon Co., Solvang, Calif., U.S.A.) liquid helium cold finger, the finger being cooled in a nitrogen flow dewar (Anger, G., Astlind, T., Petersson, L. and Ehrenberg, A., unpublished). Two microwave frequencies (8.74 and 9.32 GHz) were used, the cavity resonance being adjusted with metal cavity inserts; this shift results in a 0.75 MHz shift in the free proton frequency.

Preparation of samples

Chromatium high-potential iron–sulfur protein and *C. pasteurianum* ferredoxin were purified, and reconstituted with ^{57}Fe as previously described [3, 4]. The EPR

and ENDOR spectra of the proteins reconstituted with ^{56}Fe were indistinguishable from those of the native proteins. Samples, consisting of at least 1 μmole of protein were prepared in 2 mM Tris–Cl, pH 8.0, and concentrated by a stream of N_2 gas to a volume of 200 μl. In the preparation of oxidized high-potential iron–sulfur protein samples, care was taken to remove all traces of ferricyanide, which causes relaxation of proton ENDOR, by passage of the oxidized protein through Sephadex G-25. Reduced ferredoxin samples were prepared using $Na_2S_2O_4$ [4]. Samples of reduced *C. pasteurianum* ferredoxin in 80 % Me_2SO, were prepared in the same way as super-reduced high-potential iron–sulfur protein samples [12], except that the pH of the high-potential iron–sulfur protein solution was 9.5, and of the ferredoxin 8.0.

RESULTS

EPR results

The EPR spectra of all the samples used have appeared previously [1, 12] with the exception of *C. pasteurianum* ferredoxin in 80 % Me_2SO; the latter appears as an insert in Fig. 3 and has $g_{\parallel} = 2.06$ and $g_{\perp} = 1.94$. Replacing ^{56}Fe with ^{57}Fe ($I = \frac{1}{2}$) in these proteins results in a noticeable EPR broadening of all lines except the low-field peak of *C. pasteurianum* ferredoxin in 80 % Me_2SO; its 21 G half width at half height is increased by less than 1 G. High-potential iron–sulfur protein with its narrow EPR lines shows the greatest hyperfine broadening: at low field the half width at half height increases from 6.5 to 9.7 G and at high field the peak-to-peak separation increases from 30 to 36 G. All other resonances show noticeable but marginal broadening.

ENDOR

ENDOR (electron-nuclear double resonance) measures the tensor components describing the effective electron-nuclear hyperfine interactions. The application of this technique to iron–sulfur proteins is more extensively discussed elsewhere [1, 13].

ENDOR spectroscopy of iron–sulfur proteins [1, 13, 14] results in two types of resonances: each class of protons ($I = \frac{1}{2}$) is seen as a doublet centred at the proton Zeeman frequency (ν_p) and split by A_i, the magnitude of the hyperfine interaction (if $A_i/2 < \nu_p$). Iron, if the protein is enriched in ^{57}Fe ($I = \frac{1}{2}$), also results in a doublet for each type of iron but centred at $A_i/2$ and split by twice the iron Zeeman frequency (for $A_i/2 > \nu_{Fe}$). To separate the iron signal from the many overlapping proton resonances in the iron–sulfur proteins, one must take the difference between ENDOR spectra from ^{57}Fe ($I = \frac{1}{2}$) and ^{56}Fe ($I = 0$), these spectra being run consecutively under identical experimental conditions. The baseline is set with the radio frequency power off and small differences in sample concentration are compensated for by adjusting the relative gains for zero difference signal at either end of the iron resonance. This procedure assumes the proton resonances in ^{57}Fe are the same as they were in native or ^{56}Fe reconstituted ferredoxin (the latter two have identical EPR and ENDOR spectra). This assumption is generally valid but Scholes et al. [15] have observed in myoglobin that an iron resonance can be relaxed, hence not observed, when its resonant frequency corresponds to the free proton frequency, even if proton resonances are not observed. Similar effects may account for the absence of A_x and A_y $^{57}Fe(II)$ resonances in spinach ferredoxin [13] even though those resonances must

certainly coincide with those observed in totally deuterated algal ferredoxin [14]. Attenuation of proton and perhaps iron signals is observed in high-potential iron–sulfur protein (see below) and results in negative iron difference signals, the positive and negative portions having comparable intensities under conditions favourable for proton ENDOR (low microwave power and/or high temperature). Some attenuation, seen as a negative difference ENDOR spectrum, remains even at 2 °K and 200 mW microwave power. Possible distortions must always be kept in mind when iron and proton ENDOR resonances overlap.

ENDOR results for high-potential iron–sulfur protein

The ENDOR spectra of native and ^{56}Fe-reconstituted high-potential iron–sulfur protein are identical and are shown at three field positions (marked on the EPR inserts) in Fig. 1 (dashed lines). Note that only a broad, unstructured distribution is observed, all resolution being lost due to the large number and variety of proton

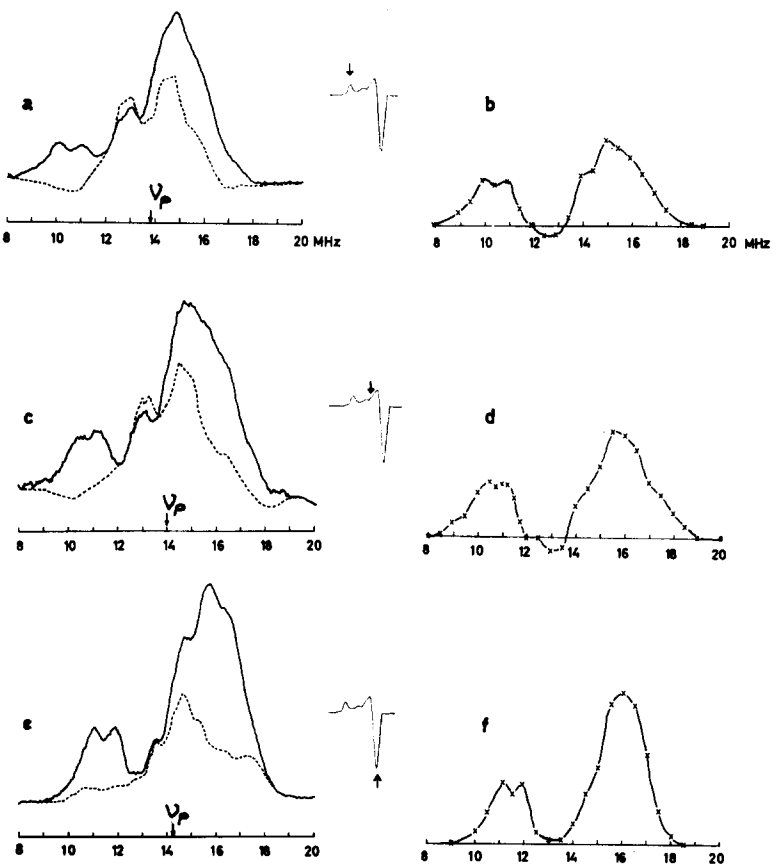

Fig. 1. ENDOR spectra of oxidized native (- - -) and ^{57}Fe-enriched (—) high-potential iron–sulfur protein with difference spectra. $T = 4.2$ °K, $P = 200$ mW, $\nu_0 = 9.32$ GHz. a) $\mathscr{H}_{\parallel}$, experimental spectra; b) $\mathscr{H}_{\parallel}$, difference spectrum; c) $\mathscr{H}_{\parallel}+75$ G ($\equiv\mathscr{H}_{\perp}-30$ G), experimental spectra; d) $\mathscr{H}_{\parallel}+75$ G, difference spectrum; e) $\mathscr{H}_{\perp}+20$ G, experimental spectra; and f) $\mathscr{H}_{\perp}+20$ G, difference spectrum.

couplings. Although this distribution is structurally centred at the free proton frequency, it need not be symmetric in intensity.

The ENDOR spectra of high-potential iron–sulfur protein reconstituted with ^{57}Fe show iron resonances which overlap with the proton resonances, the iron difference signal being maximized at very low temperature (2 °K) and maximum microwave power (200 mW). The spectra were treated as discussed previously and are shown as solid curves in Figs 1a, c, e, for field values corresponding to $\mathscr{H}_{\parallel}$, $\mathscr{H}_{\parallel}+75$ G ($\mathscr{H}_{\perp}-30$ G) and $\mathscr{H}_{\perp}+20$ G, accompanied by handcalculated difference spectra (Figs 1b, d, f). At the low-field peak, one clearly resolved doublet is observed at 10.6 MHz, the doublet being appropriately split by twice the iron nuclear Zeeman frequency (0.9 MHz). This resonance moves up to 11.4 MHz at the high-field peak giving "$A_{\parallel}$" $= 21.2\pm0.1$ MHz and "$A_{\perp}$" $= 22.8\pm0.1$ MHz. The labelling of these components is of course tentative in the light of the unexplained EPR spectra, but the axial symmetry implied by the label is justified by the observation of resolved doublets at both field positions. At intermediate field positions (Figs 1c, d) the resonance is at a value intermediate between "$A_{\parallel}$" and "$A_{\perp}$".

A second iron resonance is also observed at higher frequency but the overlapping proton resonances result in a less resolved doublet. At low field this doublet is centred at 14.5 MHz although the doublet becomes a mere inflection in the subtracted spectra and the distribution is centred at 15.3 MHz. The cross-relaxation effects of protons and iron mentioned above has resulted here in some negative ENDOR difference signal, hence it is reasonable to assume that the difference signal is attenuated on the low-frequency side. If that is the case the doublet marks the true resonance and the distribution is artificially skewed. The other alternative is that the difference is accurate, that the properly split doublet is fortuitous, and the distribution peak marks the true resonance position. This question cannot be resolved at this time so the hyperfine component is taken as "$A_{\parallel}$" $= 29.8\pm0.8$ MHz. At high field the second iron doublet and distribution are both centred at 16 MHz giving "$A_{\perp}$" $= 32\pm$ 0.2 MHz. When the cavity frequency is lowered, the free proton frequency decreases by 0.75 MHz and this frequency doublet at the high-field peak is much better resolved. The resulting difference signals from both irons agree to ±0.1 MHz, confirming the resonances as iron rather than proton effects.

"Super-reduced" high-potential iron–sulfur protein

Preliminary ENDOR experiments on super-reduced high-potential iron–sulfur protein revealed an iron difference signal only at the high-field ($g = 1.94$) peak. This resonance was essentially identical to Fig. 3 but the difference signal intensity is five times smaller, centred at 17 MHz, and peaks at 18 MHz; hence "$A_{\perp}$" $= 17.5\pm1$ MHz.

ENDOR results for C. pasteurianum ferredoxin

Fig. 2 shows the superimposed ^{57}Fe and ^{56}Fe *C. pasteurianum* ferredoxin ENDOR spectra taken at the two field extrema and one intermediate field value. The hand-calculated difference spectra accompany the experimental data and demonstrate only a single rather broad resonance. At the lowest field position (Figs 2a, b) the ^{57}Fe contribution is non-zero from 9–16 MHz, the peak occurring at 13 MHz. The resolution at 14 MHz coincides with the free proton frequency and does not

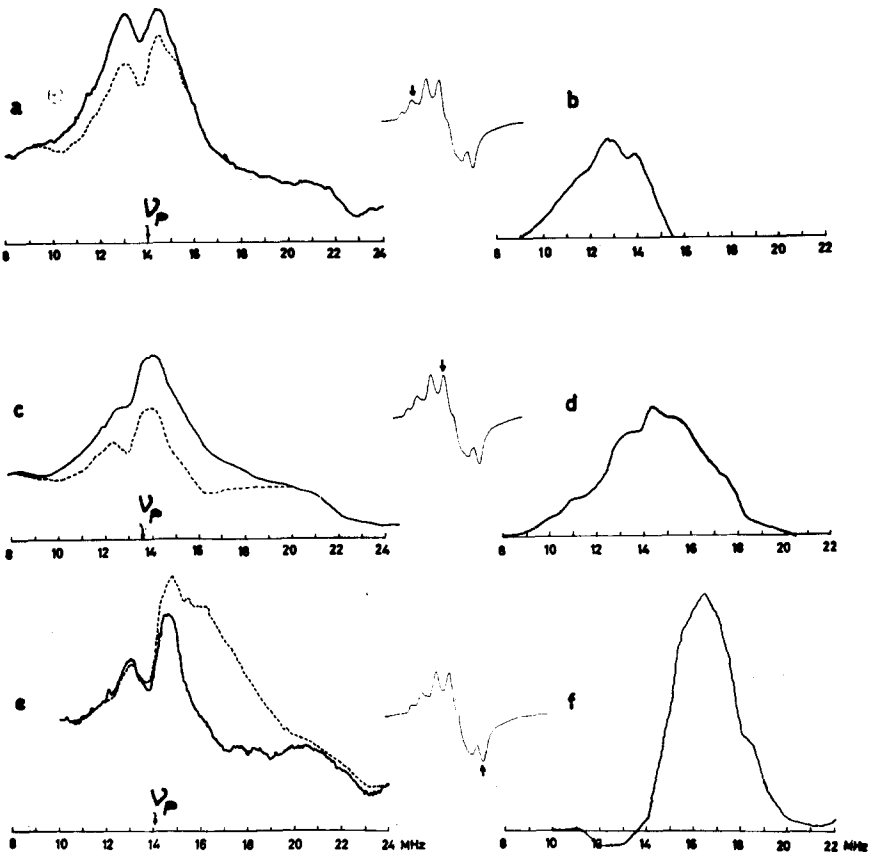

Fig. 2. ENDOR spectra of native (- - -) and ^{57}Fe-enriched (—) fully reduced *C. pasteurianum* ferredoxin. $T = 4.2$ °K, $P = 100$ mW, field positions shown on EPR inserts. a, c, and e are experimental spectra, b, d, and f are the corresponding difference spectra. Note a and b have $\nu_0 = 9.32$ GHz, all the others have $\nu_0 = 8.74$ GHz.

exist when ν_p is moved to 13.5 MHz, the distribution, however, remains centred at 13 MHz. The inflection at 12 MHz also remains, suggesting that the smallest hyperfine component may lie below the distribution peak; this question is unresolved so the average is taken with an appropriate error, i.e. "A_z" $= 25 \pm 1.5$ MHz.

At higher field (Fig. 2d) the iron resonance broadens to high frequency until at the high-field extreme (Fig. 2f) the resonance is relatively narrow (3 MHz), symmetrical and centred at 16.5 MHz. Thus, "A_x" $= 33 \pm 1$ MHz. "A_y" is presumed to lie between A_z and A_x as no resonance is observed above A_x or below A_z at intermediate fields.

The fact that no other iron resonances were observed from 4 to 30 MHz suggests that each of the eight iron atoms has approximately (within the range of the linewidth) the same spin density, or at least the same average density within the measurement time. The possibility of additional resonance(s) cannot of course be excluded considering the sensitivity of the measurement; for example a very anisotrop-

ic and hence broad resonance may not have been detected but there is no evidence from either Mössbauer spectroscopy or ENDOR to believe in any non-observed iron. The small EPR broadening excludes the possibility of any coupling larger than the one observed.

ENDOR of C. pasteurianum ferredoxin in 80 % Me_2SO

ENDOR spectra of ^{57}Fe and native *C. pasteurianum* ferredoxin in 80 % Me_2SO are shown in Fig. 3 for the EPR high-field peak. The resulting difference spectrum is essentially identical with that of the corresponding ENDOR spectrum of fully reduced *C. pasteurianum* ferredoxin (Fig. 2f); a 2.5 MHz wide distribution centred at 17 ± 0.2 MHz, hence "$A_\perp$" $= 34 \pm 0.4$ MHz. A less intense but otherwise identical difference signal was observed at field positions just below the crossing point but at the low-field peak no difference ENDOR signal was observed. As very little EPR hyperfine broadening is observed there, "$A_\parallel$" must be small, perhaps coinciding with the free proton frequency.

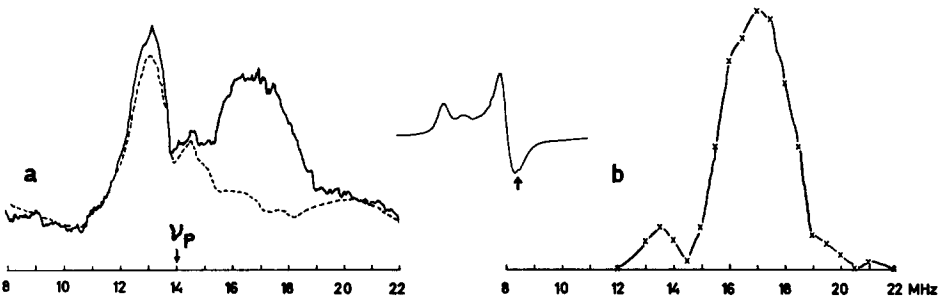

Fig. 3. ENDOR spectra of native (- - -) and ^{57}Fe-enriched (—) fully reduced *C. pasteurianum* ferredoxin in 80 % Me_2SO. $T = 4.2$ °K, $P = 200$ mW, $\nu_0 = 8.74$ GHz. Field position $\mathscr{H}_\perp + 30$ G. a) experimental spectra; and b) difference spectrum.

DISCUSSION

The present study was undertaken to determine the electronic nature of the 4-Fe and 8-Fe ferredoxins. This information is principally useful in establishing the minimum number of iron types, in estimating electron delocalization, and most importantly to provide iron hyperfine parameters essential for Mössbauer computer simulations. Only the latter can conclusively establish the valence states and electron orbital symmetries.

The ENDOR results are summarized in Table I and show that within the measurement time there are two clearly distinguishable types of iron in high-potential iron–sulfur protein and only one in fully reduced *C. pasteurianum* ferredoxin (though a heterogeneity of ± 1 MHz cannot be excluded). All of the observed iron resonances are nearly isotropic, the hyperfine components in high-potential iron–sulfur protein varying from 21.1 to 22.8 MHz and 30.0 to 32.1 MHz, and those in ferredoxin varying from 25 to 33 MHz. These anisotropies are comparable to Fe(III) in plant type ferredoxins [14] (42–51 MHz) but are very much smaller than the 13–36.5 MHz variation in the highly anisotropic Fe(II). These results are consistent with Mössbauer

TABLE I

EFFECTIVE HYPERFINE CONSTANTS IN MHz

	"$A_{\parallel}$"		"$A_{\perp}$"
Oxidized high-potential iron–sulfur protein			
Iron type I	21.2±0.1		22.8±0.1
Iron type II	29.8±0.8		32.0±0.2
Super-reduced high-potential iron–sulfur protein	?		35±1
C. pasteurianum ferredoxin in 80 % Me_2SO	?		34±0.4
	"A_z"	"A_y"	"A_x"
C. pasteurianum ferredoxin	25±2	(29±5)	33±1

data of these proteins and of the 4-Fe model compound [16] $[Fe_4S_4(SR_4)]^{3-}$. The behaviour for reduced ferredoxin can be interpreted as a delocalization of each reducing electron over the four irons of each of two identical (or nearly identical) 4-Fe clusters; this symmetrical delocalization accounts for small anisotropy and an apparent single type of iron.

Oxidized high-potential iron–sulfur protein, however, has a single 4-Fe cluster per molecule yet two types of nearly isotropic iron hyperfine couplings are detected by ENDOR. The correlation of these distinctly different couplings to the EPR spectrum is as yet uncertain since there exists no definite interpretation of the spectral features additional to the pure axial shape. Both iron resonances may result from a single cluster with $S_{\text{eff}} = \frac{1}{2}$ and an axial g tensor. If there are two EPR contributions per cluster or two types of clusters, each iron resonance may result from each of the two EPR species; this is only possible if each species has an EPR contribution at "$\mathscr{H}_{\parallel}$" and "$\mathscr{H}_{\perp}$".

The tentative results for super-reduced high-potential iron–sulfur protein and fully reduced *C. pasteurianum* ferredoxin in 80 % Me_2SO support the theory that the 4-Fe cluster is a stable three-oxidation-state unit. The EPR behaviour is consistent with an intact 4-Fe cluster, but it alone cannot exclude the possibility that the cluster has split into two 2-Fe pairs. The ENDOR data for both fully reduced Me_2SO samples, however, is inconsistent with the 2-Fe ferredoxins and is very similar to that of fully reduced *C. pasteurianum* ferredoxin (see Table I) with its intact 4-Fe clusters. Moreover, on removal of Me_2SO from these samples the proteins revert to their normal states. Proton magnetic resonance studies of oxidized *C. pasteurianum* ferredoxin in Me_2SO solutions also indicate that, although the protein is substantially denatured, the 4-Fe clusters, as detected by contact-shifted resonances, remain intact [17]. The absence of spin–spin coupling in *C. pasteurianum* ferredoxin in Me_2SO is most simply explained by an increase in the inter-cluster distance. The absence of detected ENDOR resonances at low-field positions has no definite explanation at this time, but low-intensity resonances would not have been detected in these relatively weak samples. The phenomenon may resemble that in spinach ferredoxin, discussed above, and both might be explained by cross-relaxation effects with protons.

The ENDOR hyperfine measurements for the 4-Fe clusters indicate that i) the

electron distribution on the iron atoms is nearly spherically symmetric within the measurement time (approx. $5 \cdot 10^{-8}$ s); ii) there are two types of iron in oxidized high-potential iron–sulfur protein; iii) there is only one type of iron observed in all of the fully reduced 4-Fe centres; and iv) the low magnitude of all the couplings relative to that observed in the two iron ferredoxins suggests an even greater electron delocalization onto the ligands.

ACKNOWLEDGEMENTS

This work was supported at the Biophysics Department in Stockholm by the Knut and Alice Wallenberg Foundation and by the Swedish Medical and Natural Science Research Councils, and at the Botany Department in London by the U.K. Science Research Council. The stay of R. E. Anderson in Stockholm was made possible by a fellowship from the Swedish Medical Research Council. The collaboration between the laboratories was supported by EMBO. We wish to thank Mr Torbjörn Astlind for indispensable and most skilful assistance.

REFERENCES

1 Orme-Johnson, W. H., and Sands, R. H. (1973) Iron–Sulfur Proteins (Lovenberg, W., ed.), Vol. II, Academic Press, New York
2 Gersonde, K., Schlaak, H., Breitenbach, M., Parak, F., Eicher, H., Zyorzalla, W., Kalvius, M. and Mayer, A. (1974) Eur. J. Biochem. 43, 307–317
3 Dickson, D. P. E., Johnson, C. E., Cammack, R., Evans, M. C. W., Hall, D. O. and Rao, K. K. (1974) Biochem. J. 139, 105–108
4 Thompson, C. L., Johnson, C. E., Dickson, D. P. E., Cammack, R., Hall, D. O., Weser, U. and Rao, K. K. (1974) Biochem. J. 139, 97–103
5 Phillips, W. D. and Poe, M. (1973) Iron–Sulfur Proteins (Lovenberg, W., ed.), Vol. II, Academic Press, New York
6 Poe, M., Phillips, W. D., McDonald, C. C. and Orme-Johnson, W. H. (1971) Biochem. Biophys. Res. Commun. 42, 705–713
7 Phillips, W. D., Poe, M., McDonald, C. C. and Bartsch, R. G. (1970) Proc. Natl. Acad. Sci. U.S. 67, 682–687
8 Carter, C. W., Freer, S. T., Xuong, Ng. H., Alden, A. and Kraut, J. (1971) Cold Spring Harbor Symp. Quant. Biol. 36, 381–389
9 Adam, E. T., Sieker, L. C. and Jensen, L. H. (1973) J. Biol. Chem. 248, 3987–3996
10 Carter, C. W., Kraut, J., Freer, S. T., Alden, R. A., Sieker, L. C., Adam, A. and Jensen, L. H. (1972) Proc. Natl. Acad. Sci. U.S. 69, 3526–3529
11 Evans, M. C. W., Hall, D. O. and Johnson, C. E. (1970) Biochem. J. 119, 289–291
12 Cammack, R. (1973) Biochem. Biophys. Res. Commun. 54, 548–554
13 Fritz, J., Anderson, R. E., Fee, J., Palmer, G., Sands, R. H., Tsibris, J. C. M., Gunsalus, I. C., Orme-Johnson, W. H. and Beinert, H. (1971) Biochim. Biophys. Acta 253, 110–133
14 Anderson, R. E. (1972) Ph. D. Thesis, University of Michigan Microfilms, Ann Arbor, Mich.
15 Scholes, C. P., Isaacson, R. A., Yonetani, T. and Feher, G. (1973) Biochim. Biophys. Acta 322, 457–462
16 Frankel, R. B., Herskovitz, T., Averill, B. A., Holm, R. H., Krusic, P. J. and Phillips, W. D. (1974) Biochem. Biophys. Res. Commun. 58, 974–982
17 McDonald, C. C., Phillips, W. D., Lovenberg, W. and Holm, R. H. (1973) Ann. N.Y. Acad. Sci. 222, 789–799